REPORT DOCUMENTATION PAGE

Form Approved
OMB No. 0704-0188

1. REPORT DATE *(DD-MM-YYYY)*	2. REPORT TYPE	3. DATES COVERED *(From - To)*
17102005	Journal Article	

4. TITLE AND SUBTITLE

Behavior of a Large Cylinder in Free-Fall Through Water

5a. CONTRACT NUMBER

5b. GRANT NUMBER

5c. PROGRAM ELEMENT NUMBER

6. AUTHOR(S)

Andrei V. Abelcv, Philip J. Valent, K. Todd Holland

5d. PROJECT NUMBER

5e. TASK NUMBER

5f. WORK UNIT NUMBER

7. PERFORMING ORGANIZATION NAME(S) AND ADDRESS(ES)

Naval Rescarch Laboratory
Marine Geoacoustics Division
Stennis Space Center, MS 39529

8. PERFORMING ORGANIZATION REPORT NUMBER

NRL/JA/7430-05-5

9. SPONSORING/MONITORING AGENCY NAME(S) AND ADDRESS(ES)

Office of Naval Rcsearch
800 North Quincy Street
Arlington VA 22217-5000

10. SPONSOR/MONITOR'S ACRONYM(S)

ONR

11. SPONSOR/MONITOR'S REPORT NUMBER(S)

12. DISTRIBUTION/AVAILABILITY STATEMENT

Approved for public release; distribution is unlimited

13. SUPPLEMENTARY NOTES

IEEE Journal of Oceanic engineering, Vol. 32, No. 1, January 2007

14. ABSTRACT

Abstract—This paper presents results of experimental deployment of a large instrumented cylinder of variable nose geometry and center of mass offset (CMO) in free-fall in realistic environment. Data on four tests series in the Gulf of Mexico are presented and analyzed statistically. The stochastic nature of the problem of the cylinder free-falling through water is outlined and described as an input to the subsequent impact burial prediction package. Significance of the CMO on the behavior of the cylinder is underlined. Influence of the release conditions on trajectory is discussed and found to affect the behavior of the cylinders only in the

15. SUBJECT TERMS

Cylinder dynamics, free-fall, hydrodynamics, quasi-stable, trajectory, terminal conditions

16. SECURITY CLASSIFICATION OF:			17. LIMITATION OF ABSTRACT	18. NUMBER OF PAGES	19a. NAME OF RESPONSIBLE PERSON
a. REPORT	b. ABSTRACT	c. THIS PAGE			Andrei Abelev
Unclassified	Unclassified	Unclassified	UU	11	19b. TELEPHONE NUMBER *(Include area code)* 202-404-1107

Behavior of a Large Cylinder in Free-Fall Through Water

Andrei V. Abelev, Philip J. Valent, and K. Todd Holland

Abstract—**This paper presents results of experimental deployment of a large instrumented cylinder of variable nose geometry and center of mass offset (CMO) in free-fall in realistic environment. Data on four tests series in the Gulf of Mexico are presented and analyzed statistically. The stochastic nature of the problem of the cylinder free-falling through water is outlined and described as an input to the subsequent impact burial prediction package. Significance of the CMO on the behavior of the cylinder is underlined. Influence of the release conditions on trajectory is discussed and found to affect the behavior of the cylinders only in the first 3.5 m of free-fall in water. Beyond this depth, quasi-stable (in the mean sense) conditions are achieved. Effects of three different nose shapes—blunt, hemispherical, and chamfered—on cylinder behavior are analyzed and found to have a pronounced influence on the fall trajectory. The blunt nose shape appears to be hydrodynamically most stable in free-fall. Apparent periodicity in motions of all cylinders were noted and were found to be the function of the CMO and nose shape primarily. Implications of these and other findings on modeling and impact burial predictions are discussed.**

Index Terms—**Cylinder dynamics, free-fall, hydrodynamics, quasi-stable, trajectory, terminal conditions.**

I. Introduction

THE main objective of this paper is to collect, systematically analyze, and quantify the experimental data on the complex 3-D behavior of an instrumented cylinder during free-fall in water and sediment. This knowledge is required for estimating the amount of burial of cylindrical objects in soft seafloor marine sediments, and depends on our ability to quantify two main categories of data. One category includes accurate description of the characteristics of the bottom sediments, pertaining to the high strain and high strain rate deformation. This knowledge also needs to reflect the natural variability of these parameters in both spatial and temporal domains. Information on the linear and angular velocities and orientation of the free-falling cylinder at the point of impact with the sediment surface represents the second category of the input information required for the prediction of the penetration burial.

Manuscript received April 25, 2005; revised September 16, 2005; accepted October 17, 2005. This work was supported by the U.S. Naval Research Laboratory (NRL) Base Program under Mine Burial Project, managed by Dr. M. Richardson, under Program Element 62435N. The Corpus Christi experiment was supported by the U.S. Office of Naval Research (ONR) Mine Burial Program, formerly managed by Dr. R. Wilkens, now managed by Dr. T. Drake and Dr. B. Almquist, under Program Elements 61153N and 62435N.

Guest Editor: R. H. Wilkens.

A. V. Abelev was with the University of Southern Mississippi, Stennis Space Center, MS 39529 USA. He is now with the U.S. Naval Research Laboratory, Stennis Space Center, MS 39529 USA (e-mail: aabelev@nrlssc.navy.mil).

P. J. Valent and K. T. Holland are with the U.S. Naval Research Laboratory, Stennis Space Center, MS 39529 USA.

Digital Object Identifier 10.1109/JOE.2007.890938

Behavior of cylindrical bodies during free-fall has been modeled in the past [1], [2]. More recent developments, involving improved and more realistic approaches, have been reported [3], [4]. Accurate numerical modeling depends in large on the ability to describe the complex 3-D dynamic behavior of a cylinder in free-fall and requires proper accounting for all the forces acting on the falling cylinder. Under ideal conditions, the water column is usually represented as a semi-infinite space with isotropic and constant properties. These properties typically include temperature, salinity, and density. Under these conditions, it has been shown that an idealized cylindrical body, free-falling through the water, could reach a number of stable or quasi-stable motion patterns [1]. Depending on the geometry and the distribution of mass, a range of trajectories can be expected. Several distinct patterns have been experimentally observed and were identified as straight, spiral, flip, flat, and seesaw. A single trajectory may consist of a single pattern or any number and any combination of these motions. Each one of these patterns appears to be stable and, if the cylinder enters a particular pattern, it will remain in this pattern until a sufficient disturbance is applied to the moving body.

For the first time, a full-scale instrumented cylinder has been released in a realistic field setting. The instrument data is used to characterize the statistics of the dynamic behavior exhibited by this cylinder. In Section II, we describe the instrumented cylinder and its deployment. Then, in Section III, we present the statistical characterization of the observational data. These results suggest that after a short initial period, the free-falling cylinders reach a quasi-stable state, with oscillations about a mean. Finally, in Section IV, we discuss the implications for impact burial prediction and, in Section V, we summarize our findings.

It is important to underline that the overall goal is to be able to predict the amount of burial of the cylindrical bodies in soft seafloor sediments. Thus, the accurate description of the conditions of the cylinder at the point of initial contact with the sediment, in the statistical sense, is crucial to the ability to predict the amount of penetration. Actual modeling of the mechanisms of the cylinder free-fall through water and penetration into the sediment is beyond the scope of this paper.

II. Experimental Setup, Equipment, and Procedures

A. Instrumented Cylinder, Data Acquisition, and Data Processing

The instrumented cylinder measures 0.53 m in diameter and 2.40 m of length, yielding a length-to-diameter ratio of 4.5. Its weight in air is approximately 10 kN and its weight in water (seawater) is about 4.9 kN (mass of 1070 kg). The cylinder designed for this paper had an adjustable position of the center of

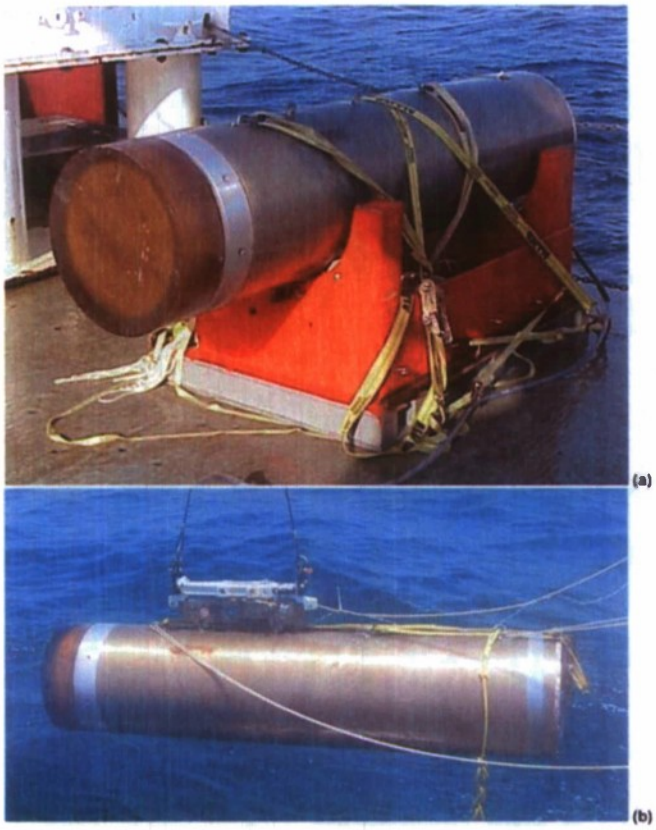

Fig. 1. General view of the instrumented cylinder with the blunt nose (a) attached in the cradle and (b) before release.

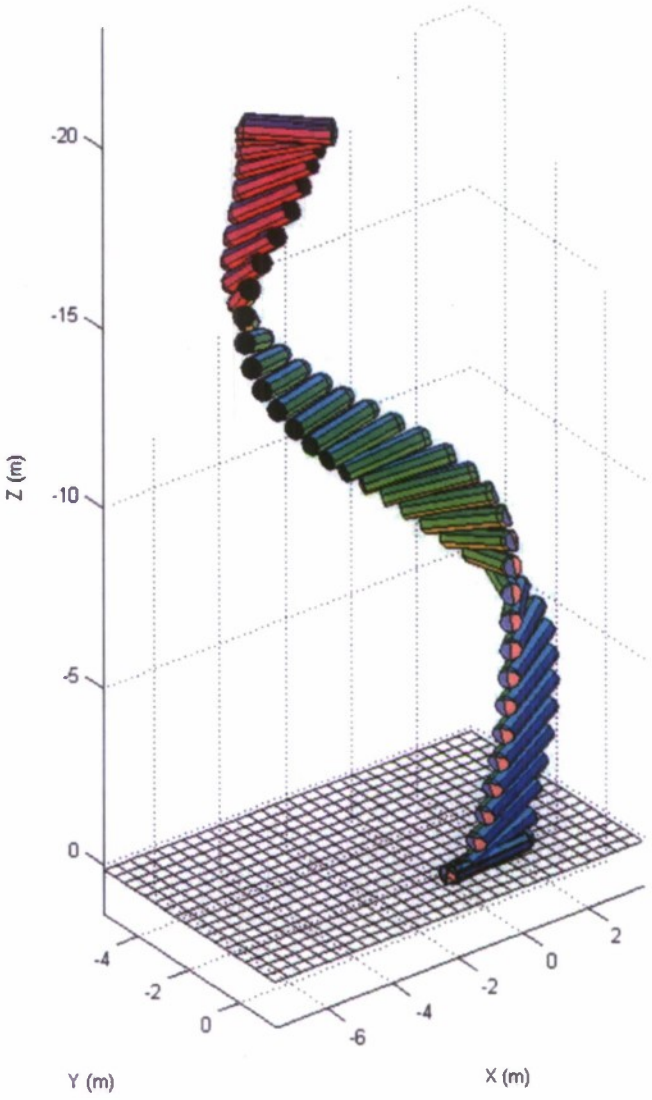

Fig. 2. Typical calculated trajectory of the instrumented cylinder in free-fall. The cylinder is outfitted with the chamfered nose.

mass (CM) relative to the center of volume (CV), along its main axis. Two configurations of the center of mass offset ratio (CMO $= (\mathrm{CM} - \mathrm{CV})/L$) were tested: 0.05 and 0.02, where L is the overall cylinder length. In both cases, the CM was located forward of the CV. Three interchangeable nose shapes were manufactured: blunt, hemispherical, and chamfered. Fig. 1 depicts the instrumented cylindrical shape, strapped to a cradle and with the blunt nose mounted.

The internal instrumentation, placed in a sealed container inside the cylinder, included a set of accelerometers measured along three orthogonal axes. These accelerometers had three different ranges: 2.5, 4, and 10 g. Additionally, a triaxial fiber-optic gyro (FOG) measured the angular rotation rate around the three orthogonal axes, collinear with the axes of the accelerometers. The internal instrumentation also included a power source, a signal acquisition and conditioning unit, and a fast access memory storage device. Details of this design can be found in [5], [6], and [7].

An upgraded and expanded version of the data processing software, first described in [8], was developed. The raw data, which included variations of the components of local (cylinder's coordinate system) accelerations and angular rotation rates with respect to the elapsed time was analyzed. First, a transformation was performed from the local (cylinder) coordinate system to the fixed global system, using the Euler aerospace rotation sequence. The effects of gravity were then removed and the resulting values of accelerations and angular rotation rates were integrated to obtain a set of global (in addition to local) velocities, displacements, and angular changes as functions of the elapsed time. Calculating from its initial state, with the cylinder suspended from the ship's winch, forward processing yielded somewhat ambiguous results and was replaced with the reversed integration from the cylinder's final position at rest, embedded in the sediment, backwards. The reverse integration method produced more realistic and consistent description of the water column and sediment penetration trajectories. The advantage of this approach was in the fact that the conditions at rest are easier and more accurately defined than those at the time of release. Comparisons between the forward and reverse integration schemes showed only minor errors in the overall calculated displacements, accumulated over the entire trajectory.

The data postprocessing routines resulted in a set of data that allows the analysis of many individual components of the process of free-fall and penetration into the sediment. Fig. 2 represents an example of a typical visualization of the calculated trajectory of the cylinder during free-fall. Accurate and detailed

TABLE I
TESTS SORTED BY NOSE SHAPE, RELEASE ANGLE, AND CMO

Blunt nose	48
Hemispherical nose	42
Chamfered nose	23
Air released	42
Water released	71
Horizontal releases	28
Releases at 31°	30
Releases at 4.5°	55
$(CM - CV)/L = 0.05$	58
$(CM - CV)/L = 0.02$	55

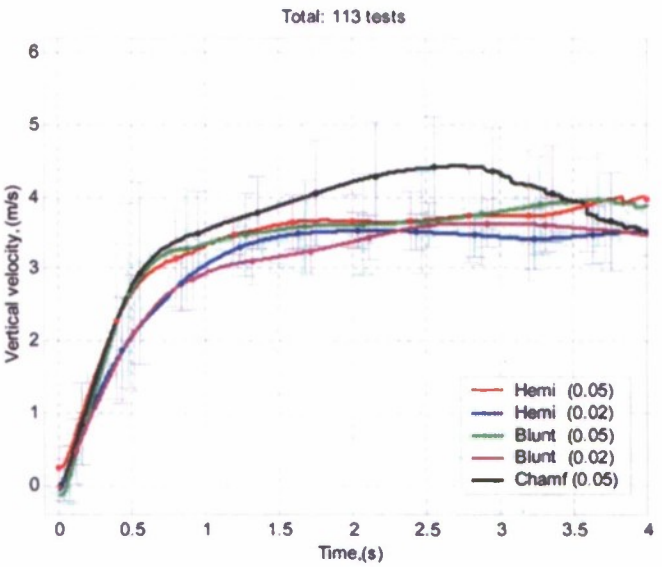

Fig. 3. Averages and STDs plotted as error-bars for all drops, sorted by nose shape and CMO.

analysis of various components of acceleration also allowed for estimating the initial point of contact of the cylinder with the sediment floor. This point was characterized by a sharp spike in one or more components of the acceleration. The sensitivity of the instruments and the high rate of data acquisition allowed for a relatively accurate determination of this instant. This determination was important for separating the two phases of the free-fall: in-water and in-sediment.

B. Testing Procedures

The data reported in this paper was obtained during four cruises. These cruises included the January 2002 cruise on board R/V Pelican, near Cocodrie, LA (labeled P02 hereafter), May 2002 cruise on board R/V Gyre, near Corpus Christi, TX (G06), and two cruises on board R/V Pelican near East Bay, LA, in June 2003 (P03) and May 2004 (P04), respectively.

Each of these trips included a series of drops with varying cylinder nose configurations, CMO, and initial conditions. The first three cruises deployed a cylinder with CMO = 0.05 and the last one, P04, with CMO = 0.02. Release medium was also varied with some of the cylinder deployments performed from the air, usually only a small height above the water surface, and some others released from the fully submerged position of just below the water surface. Additionally, the initial inclination (pitch) was changed by using different harness arrangements: horizontal and at 31° nose down during P02, G06, and P03 cruises and approximately 5° nose down during the P04 cruise. Table I summarizes the number of tests performed, broken down by the nose shape, release medium, inclination, and CMO.

The testing sequence proceeded according to the following order. First, the internal instrumentation of the cylinder, resting in its cradle, was initialized. The cylinder was then suspended by either the harness or from the bomb release [as shown in Fig. 1(b)], brought to the desired elevation above or below the water surface and released. Generally, a 1/4-in locating line was attached to the cylinder and trailed it to the bottom. This line was necessary for the subsequent location of the cylinder by the divers in near-zero visibility at the sea bottom encountered in all deployment areas. The divers followed this line to the cylinder, located it on the bottom, and measured its final orientation, including the resting angle, and the elevation above the mudline. Additionally, cylinder heading was recorded by the divers using a small compass with storage memory. During the later cruises (P03 and P04), and as a result of accumulated experience, the measurements of final inclination and heading were not taken by the divers as these values could be inferred from the internal cylinder instrumentation with greater accuracy.

To confirm the calculated trajectory of the cylinder, including the lateral travel from the point of release to its resting position on the seafloor, a small tethered metal weight ("stake") was also released just before the cylinder deployment. The divers then located the stake on the bottom and measured the distance from the stake to the cylinder and the compass heading of this direction to produce a complete set of data that allowed for the computation of the overall lateral travel of the cylinder. The ambient current profile was also measured using an acoustic Doppler current profiler. Analysis of these data showed only minor lateral flows that were considered too small to influence the trajectory of the massive cylinder to any significant degree. Comparison of the diver measured and instrumentation processed data showed good agreement in all those deployments where diver measurements were available. Some equipment difficulties prevented the divers from measuring accurately the headings and the inclinations of the cylinder in some drops. Again, as a result of accumulated experience, the "stake" deployment was abandoned during the later cruises, as the information thus collected could be inferred with greater accuracy from processing the cylinder data or was otherwise inconsequential to the analysis performed.

Another change included replacement of the 1/4-in locating line during the P04 cruise with a 1-in stranded synthetic line. Care was taken to ensure that this larger diameter line would add minimum line drag during deployments, which could potentially influence the trajectory. Comparisons between drops with and without the 1-in line, otherwise performed under identical conditions, showed no perceptible difference in the trajectory or any other component of the cylinder behavior during

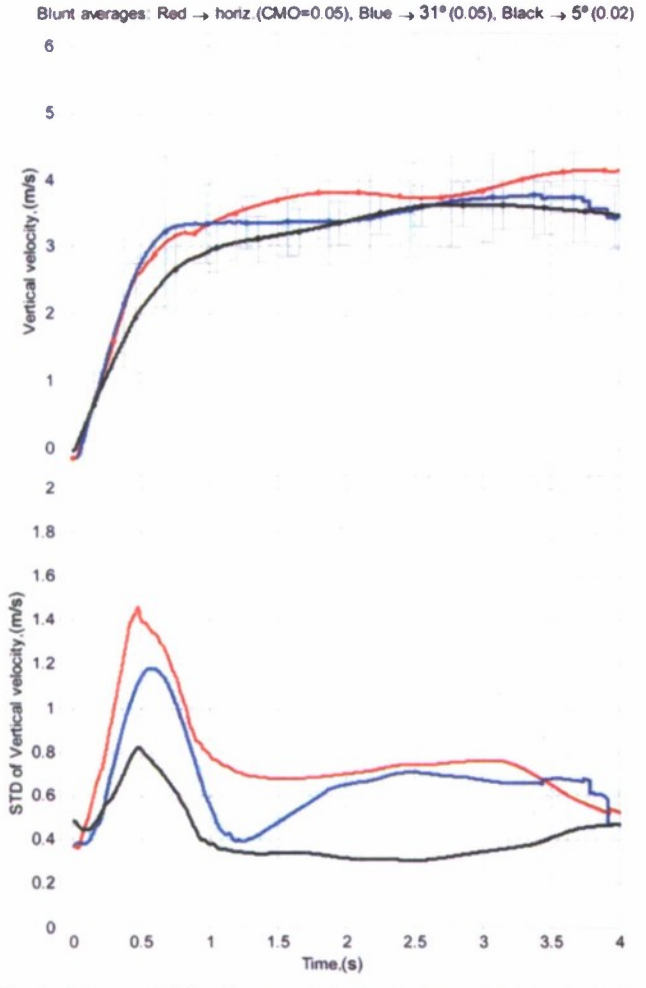

Fig. 4. Means and STDs of the vertical velocity time series for cylinder deployments with blunt nose, sorted by release angle.

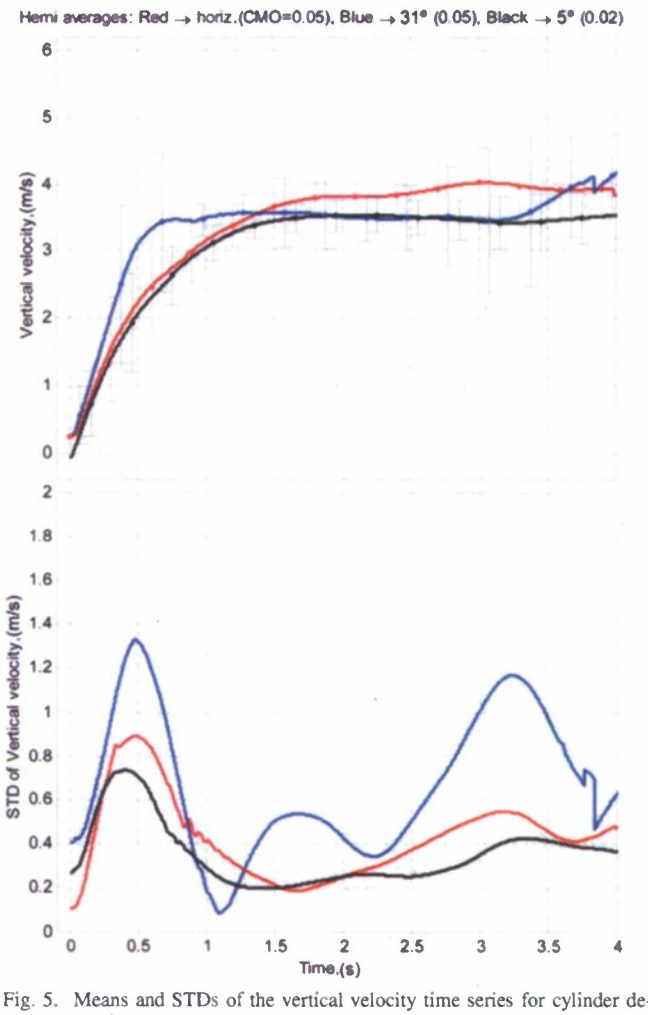

Fig. 5. Means and STDs of the vertical velocity time series for cylinder deployments with hemispherical nose, sorted by release angle.

free-fall through water. The synthetic line was very nearly neutrally buoyant (when submerged), apparently generating only small added drag forces during the fall, relative to the dominant gravitational component of the massive cylinder.

III. Experimental Results

A. General

The set of data collected during the four cruises reported herein allows for detailed evaluation of the complex dynamic mechanism of a free-falling cylinder. As evidenced from Fig. 2, and other calculated trajectories, the motions of the cylinder are highly 3-D. The corresponding cylinder state, at the point of contact with the sediment, may be described by nine variables, including three components of velocity, three orientation angles, and three angular rotation rates. The dimensionality of the system can be reduced by considering the symmetries of the problem, i.e., axisymmetric body impacting the half-space, recalling that the overall goal is predicting the amount of cylinder penetration. In this case, the number of variables reduces to six: three velocity components, pitch, and two angular rotation rates. Further reductions are possible (keeping only four variables), if the impact of the cylinder on the bottom is considered using a 2-D model. Here, only two velocity components are of interest, vertical and horizontal, as well as one inclination angle (pitch) and one angular rotation rate. This approach is typical of cylinder burial prediction models. Since one of the goals of this investigation is to provide an input for the existing impact burial prediction software, which is 2-D, the results presented herein will address primarily those degrees of freedom of the moving cylinder that are the required inputs. The following components of the cylinder motion are thus of primary interest: vertical velocity, horizontal velocity in the plane of the cylinder, angular rotation rate (in the plane of the cylinder), and the pitch. The "plane of the cylinder" refers to the plane formed by the cylinder's main axis and the vertical.

The average depths encountered at the testing locations were approximately 15 m at East Bay, LA (P03), 16 m at Cocodrie, LA (P02) and East Bay/Garden Island, LA (P04), and about 20 m off the coast of Corpus Christi, TX (G06). Calibration and testing of any mine burial predictive algorithm would require knowledge of the conditions at impact with the sediment. The data available from these cruises, however, represent not only the information necessary to drive the predictive software at the two actual depths recorded but also everywhere else, from the point of release and until that maximum depth. The results of the experimental drops would be valid if the sea bottom was encountered at any depth within this interval.

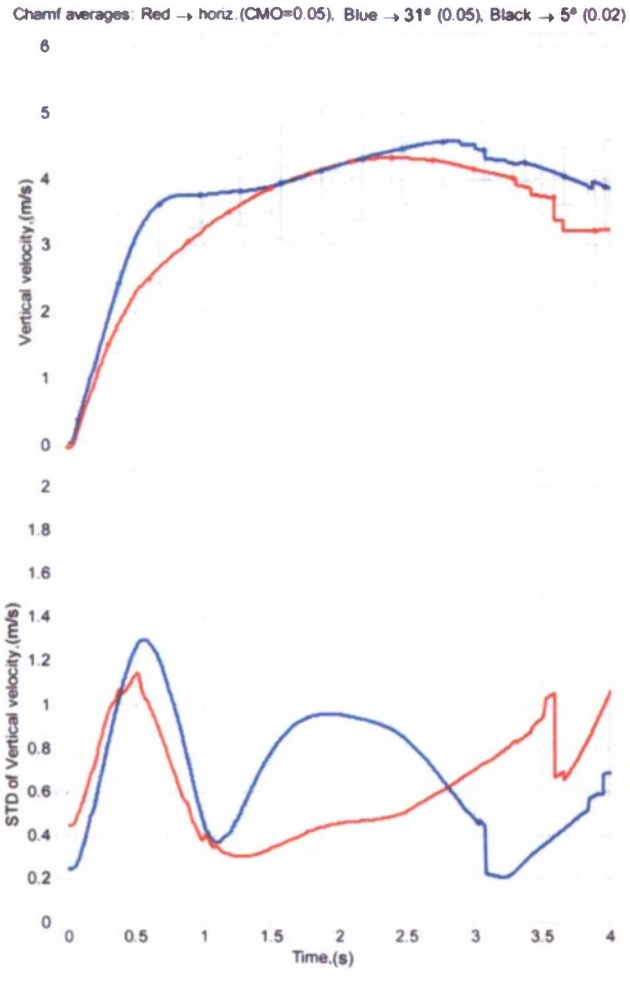

Fig. 6. Means and STDs of the vertical velocity time series for cylinder deployments with chamfered nose, sorted by release angle.

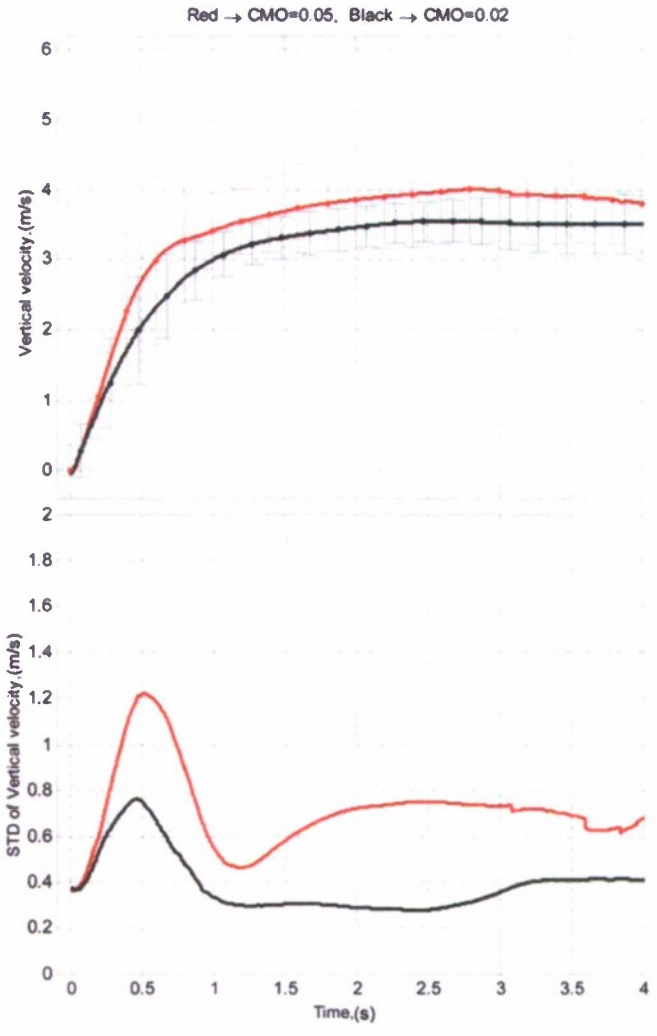

Fig. 7. Mean and STD of the vertical velocity, sorted by the CMO ratio.

B. *Vertical Velocity Variations*

The vertical component of velocity (V_Z) at impact with the sediment is one of several important factors controlling the final burial depth of a cylindrical object. The variation of V_Z with elapsed time is presented in Fig. 3. The data are represented by means and error bars [representing the standard deviation (STD)], grouped according to nose configurations—blunt, hemispherical, and chamfered—and by the CMO ratio (0.05 and 0.02). These averages were calculated based on the total of 113 deployments of the instrumented cylinder. The highly stochastic nature of the cylinder free-fall is evidenced even from these averaged values and is particularly apparent when examining the collection of all the individual drops (not shown here for clarity). As will be shown later, the stochastic nature of the problem is manifested in all the dynamic components analyzed here.

It should be pointed out that the values of the vertical velocity are not necessarily precisely zero at the time of release due to the ship's motion. The internal cylinder instrumentation (including postprocessing) records the actual movements of the body with respect to the earth-fixed coordinate system. These motions, naturally, include the ship's heave, sway, and yaw. Sea conditions during the G06 cruise were significantly more disruptive than those at any of the other test sites visited, resulting in larger deviations from the mean of all the dynamic parameters, including the vertical velocity.

The variation of the mean and the STD of the vertical velocity with time as a function of nose geometry and CMO are shown in Figs. 4–6. Analysis of these figures suggests that the mean values of the vertical velocity attain a constant value after about 1–1.5 s from the moment of release. All releases were done from less than 1 m above or below the water surface. This travel time corresponds to a maximum water depth of about 3.5 m. From this point on, the mean vertical velocity remains reasonably constant at about 3.5–4.0 m/s. This has already been observed by the authors analyzing a small subset of the data presented here and reported earlier in [5] and [6]. This observation holds for all the nose geometries and the CMOs examined.

The analysis of the changes in variance of the vertical velocity by nose shape (Figs. 4–6) reveals that after achieving the condition of this pseudoterminal mean velocity (vertical), the blunt nose shape results in the smallest amount of variation about the mean, and the chamfered nose results in the largest. The reason for this behavior could be due to the blunt nose geometry being a more hydrodynamically stable configuration in both axial- (nose

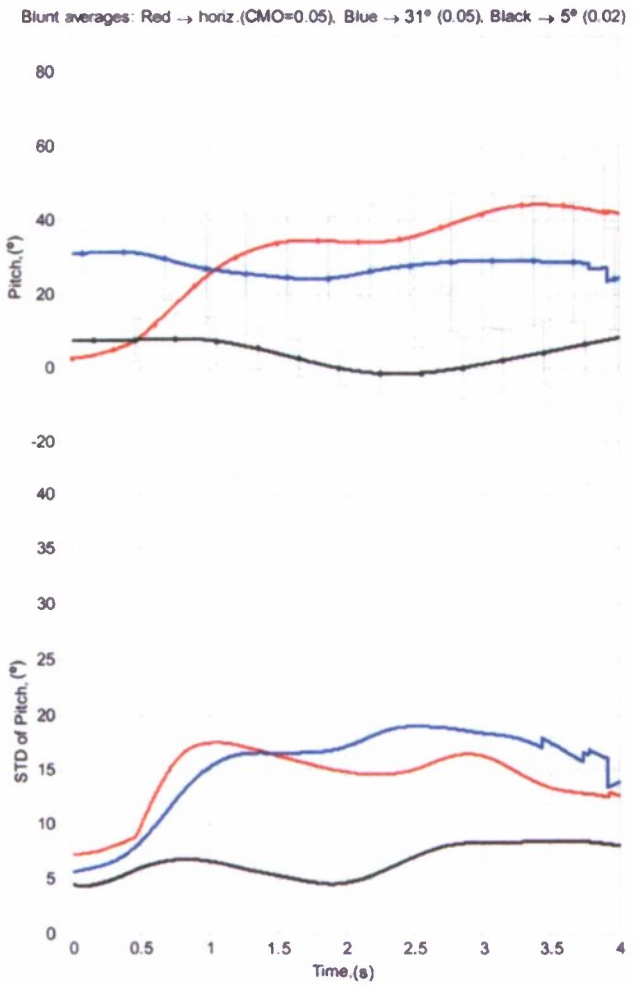

Fig. 8. Means and STDs of the pitch angle time series for cylinder deployments with blunt nose, sorted by release angle.

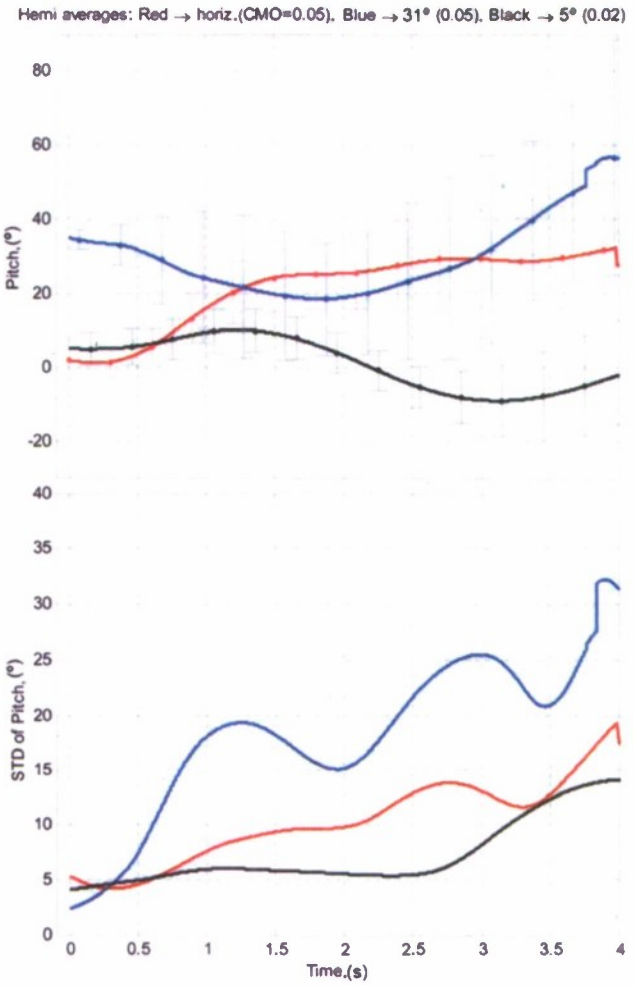

Fig. 9. Means and STDs of the pitch angle time series for cylinder deployments with hemispherical nose, sorted by release angle.

forward) and cross-flow, tending to preserve the instantaneous orientation rather than changing it. Hemispherical and, especially, chamfered nose shapes, represent conditions of a more likely rapid reorientation of the cylinder during free-fall, thus impacting values of the velocity components.

Fig. 7 represents the differences in vertical velocity behavior of all cylinders tested with two CMO ratios: 0.05 (more nose-heavy) and 0.02 (more centrally weighted). The mean vertical velocity of the more nose-heavy configuration reaches about 4 m/s as opposed to about 3.5 m/s for the second configuration (CMO = 0.02). The STD of the more centrally weighted cylinders, regardless of the nose configuration or release conditions, is about half of that of the more nose heavy shapes. This is an indication that more centrally weighted cylinders assume the orientation of broadside to the flow quicker and maintain it longer throughout the fall.

C. Pitch Variations

Vertical velocity and pitch are not independent variables, which is also evident from the examination of individual drops (see further comments in Section IV). These variables, however, are analyzed on individual basis in this paper, as they serve as separate and distinct inputs to the sediment impact penetration model currently in use.

Figs. 8–11 present the variability in pitch, sorted, as the vertical velocity before, by the nose shape (blunt, hemispherical, or chamfered), release angle (horizontal, 5°, and 31° nose-down), and the CMO (0.05, 0.02). We observe, as before, that the release conditions (initial pitch and release altitude—above or below the water surface) influence the trajectory only for the first 1.5 s at most, representing a water-column travel of less than 3.5 m. After 1.5 s, the means and the variances of the pitch angle remain quasi-stable, with largest fluctuations in the STD time series of less than 10°. The variance appears to increase progressively from the blunt shape to hemispherical and to the chamfered. This effect could be explained partially by the degree of influence the particular nose geometry has on the local flow patterns developing at the front of the cylinder. This flow creates larger torques with hemispherical rather than blunt shapes. The chamfered shape, by virtue of having a single plane at a 45° angle to the cylinder axis, is most erratic in its trajectory. Sudden changes in this trajectory appear to be caused by the current orientation of the chamfer surface, relative to the principal velocity vector. A good example of the effects of the chamfer plane is shown in Fig. 2. Note that the fluctuations of the means and

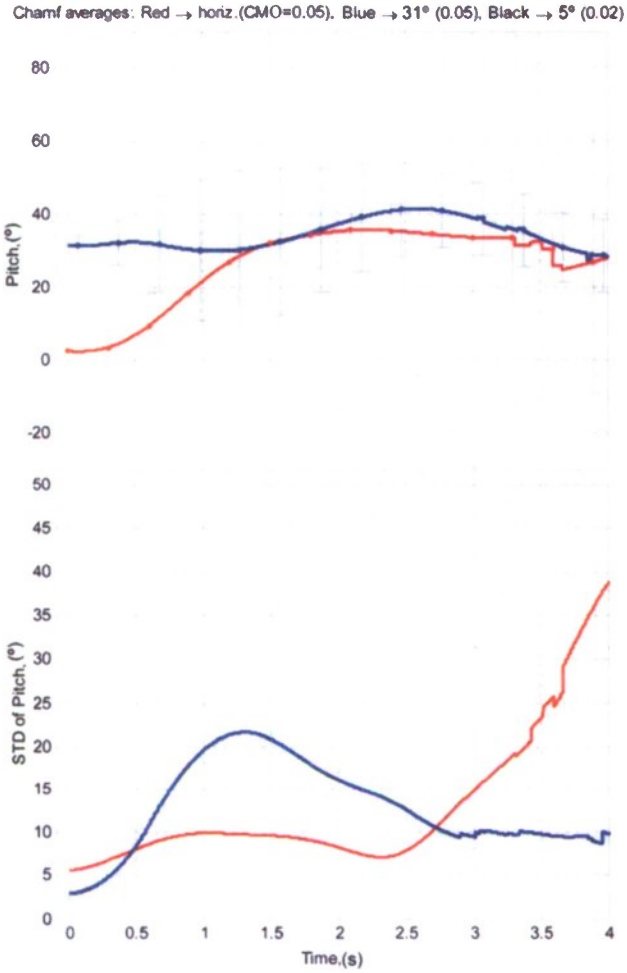

Fig. 10. Means and STDs of the pitch angle time series for cylinder deployments with chamfered nose, sorted by release angle.

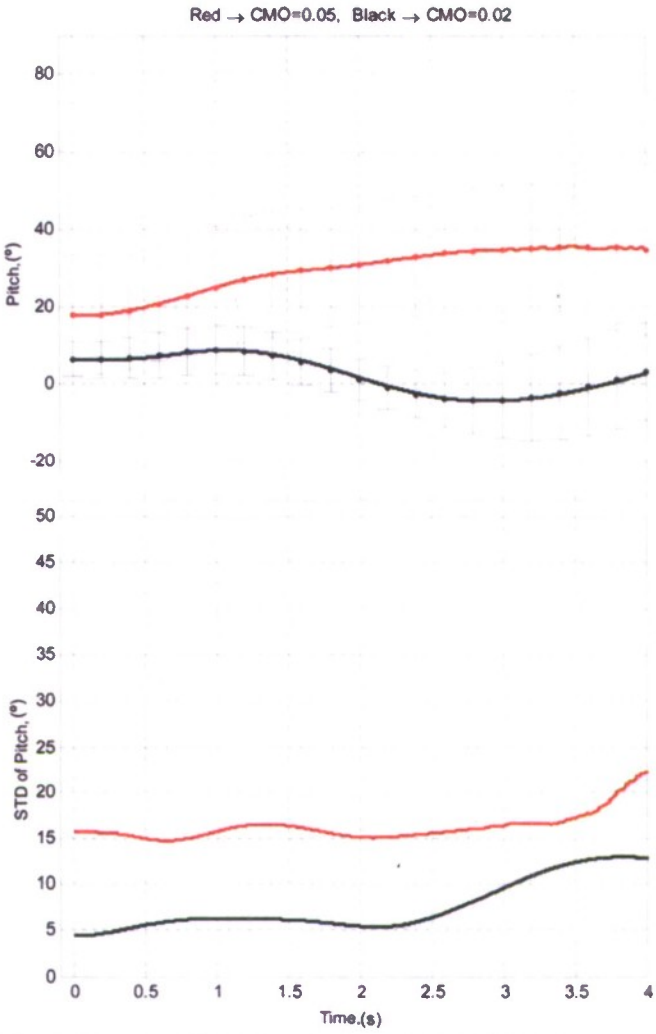

Fig. 11. Mean and STD of the pitch angle, sorted by the CMO ratio.

the STDs after 3.5 s result from the decreased number of data sets available for averaging—G06 was the only site with water depths greater than 16 m. Averaging over progressively smaller number of drops creates the effect of increased variability.

The effects of the CMO on the variability of the pitch angle are clearly shown in Fig. 11. The shapes with larger CMO (0.05) attain a relatively stable mean of about 30° with STD of about 15° and those with CMO =0.02, about 0° and 8°, respectively.

D. In-Plane Horizontal Velocity and Angular Rotation Rate Variations

The horizontal component of velocity (in the plane of the mine) and pitch rate are the other two parameters of interest, experimental description of which is needed for input into the sediment penetration prediction model. The experimental evidence on their evolution through the fall is shown in Figs. 12–14. No significant difference in behavior is observed as a function of the nose geometry of the cylinder or release conditions; however, the CMO has significant influence on the lateral velocity. Only data on the blunt nose are presented in this paper (Fig. 12, note: negative values represent forward velocity). Hemispherical and chamfered configurations showed nearly identical behavior as the blunt and are omitted herein. It appears that the fluctuations

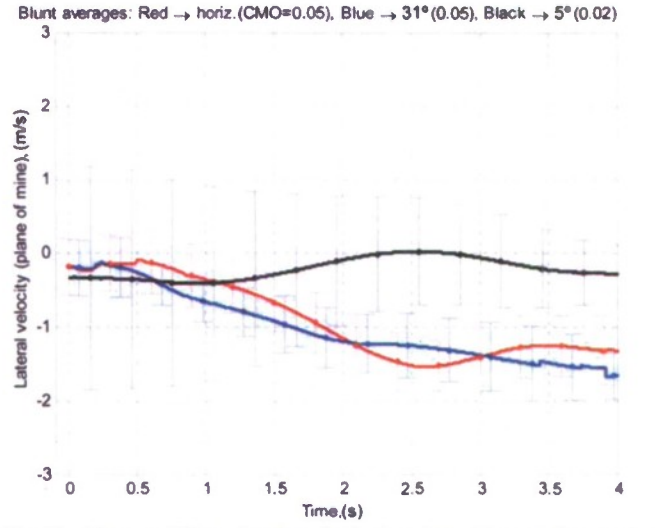

Fig. 12. Means and STDs of the lateral velocity (plane of the cylinder, negative in the forward direction) time series for cylinder deployments with blunt nose, sorted by the release angle.

of the horizontal velocity (in the vertical plane of the cylinder) persist the longest after release—as long as 2.5 s. Most dynamic

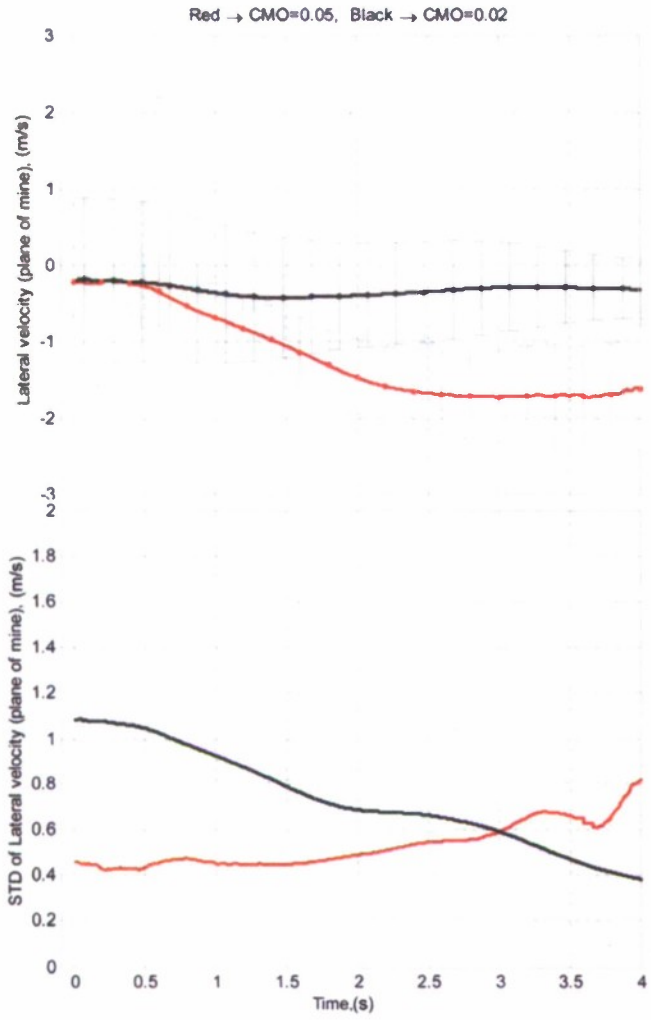

Fig. 13. Mean and STD of the lateral velocity (plane of the cylinder, negative in the forward direction), sorted by the CMO ratio.

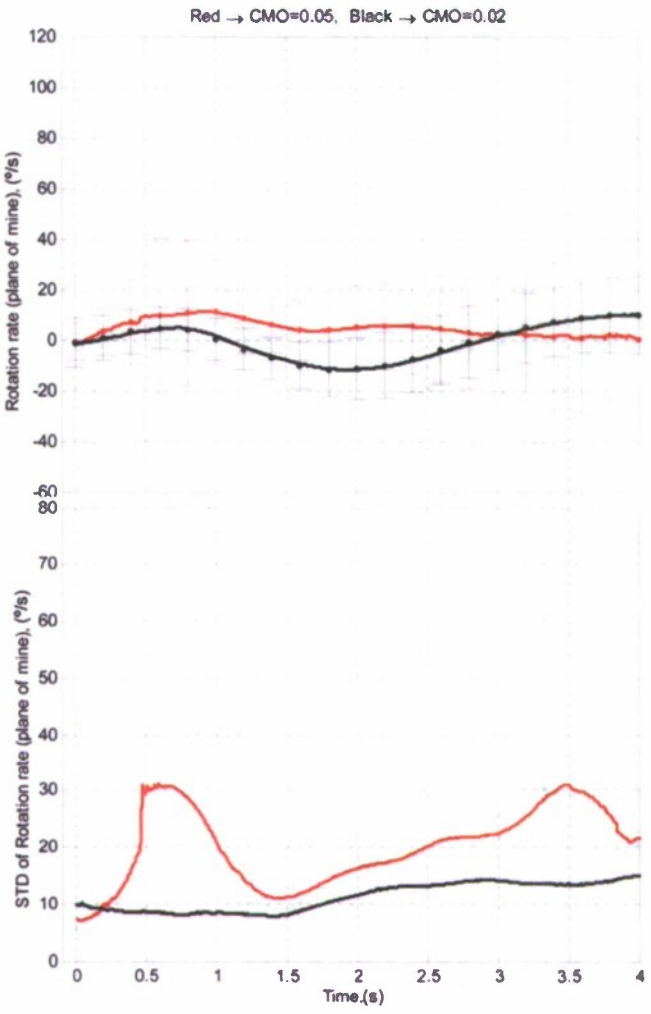

Fig. 14. Mean and STD of the angular rotation rate (plane of the mine axis and the vertical), sorted by the CMO ratio.

components stabilize (in the mean sense) at 1.5 s into the fall, as has been shown before. The average values of this velocity component at the mean stable stage are 1.7 m/s for CMO = 0.05 and 0.3 m/s for CMO = 0.02. The average values of the STDs for this time increment (> 2 s) are almost identical for the two CMOs: 0.6 m/s.

The variations of the pitch rate are shown in Fig. 14. All means are unbiased and congregate near zero. No obvious dependence on the release conditions, nose configuration, or CMO is observed. The initial spike in the STDs time series may be explained by the fact that these values were calculated on all the drops, including the air drops at 31° initial pitch (only for CMO = 0.05). The cylinders released in this configuration would impact the water surface at about the same angle (31°) and will therefore receive an immediate torque due to uneven submergence. This effect will then quickly dissipate as a result of the drag forces on the cylinder. The STD for the higher CMO is larger than that for the smaller CMO by a factor of one-half to two. The variance in pitch rate for the drops with the blunt configuration is smaller than that for hemispherical and chamfered noses. This is probably due to the before noticed effect of added hydrodynamic stability of cylinders with the blunt nose.

One other interesting variable to observe is the amount of lateral excursion or distance traversed by the free-falling cylinder from the point of release in the horizontal plane. The knowledge of the ratio of possible maximum lateral to the vertical travel of the cylinder from its release point may have a variety of implications in situations of interest to the U.S. Navy and the Homeland Security Department. Analysis of Fig. 15 shows that, although the means for the CMO = 0.02 are only slightly larger than for CMO = 0.05, the STD is about twice as high. This implies that the maximum likely lateral excursion of the cylinder from its initial release point may be on the order of 1/2 of the depth traversed for the more nose heavy cylinders and up to about 2/3 of the depth for the more centrally weighted cylinders. This likely maximum is inferred from the combined mean and STD values of the lateral excursion, as plotted in Fig. 15, and is distinguished form the comparison of the means only.

IV. Discussion

A. *Quasi-Stable Conditions and Water Entry*

It has been shown that all dynamic parameters examined in this paper, as well as additional variables that define the cylinder motions in the horizontal plane, attain quasi-stable

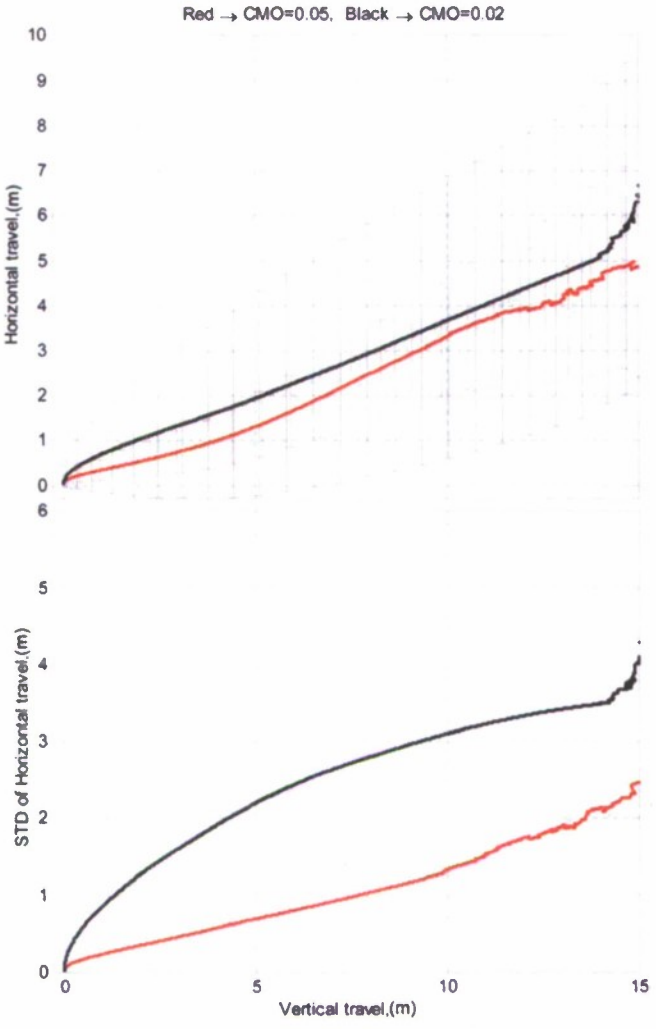

Fig. 15. Mean and STD of the horizontal travel versus mean vertical travel, sorted by the CMO ratio.

states at some point during the fall. The choice of this point is somewhat arbitrary but appears to occur at about 1.2 s after the release, on average for all variables. Since all the deployments were made at most 1 m above or below the water surface, this time of fall corresponds to about 4-m depth at the greatest. From this instant on, all the components of linear and angular velocities and rotations can be viewed as quasi-constant (mean sense only) with rather large deviation from the mean for most variables examined. The detailed list of means and STDs of the quasi-stable means of all variables examined are presented in Table II. The averaging was done for the time interval from 1.2 to 4 s after release. Erratic behavior of some of the means beyond 4 s was not included in this averaging procedure as it was mostly the result of the decreasing number of drops participating in the calculations of the means and STDs, due to the cylinder reaching the seafloor shortly after 4 s for 103 of the 113 drops.

The fact that the cylinder dynamic parameters can be considered quasi-stable after certain minimum depth is important in predicting impact burial of cylinders in soft marine deposits. As seen in Table II and Figs. 3–14, the variances of all the variables considered during this quasi-stable state are quite large. The information on the means presented is, however, valuable, given the very intrinsic nature of the sources of this variability. These sources include inhomogeneities in the temperature, density, and salinity of the water, and lack of precise information about constantly varying local currents throughout the entire water profile at the drop location, all of which influence the trajectory of the cylinder in the free-fall. Cylinders in the free-fall can assume one of several hydrodynamically stable modes of the fall [1]. These patterns include lateral slide, downward spiral, glide in the direction transverse to the vertical plane of the cylinder, seesaw motions, etc. Accurate modeling of each one of these is underway [3]. Practically, however, the cylinder may switch from one pattern to another at any time as a result of the various disturbances or perturbations. Given the practical inability to fully describe these perturbations, accurate deterministic modeling of individual drops may not be feasible. It is thus perceived that the statistical analysis of the accumulated experimental evidence may be used to calibrate the stochastic implementations of these models or serve as a direct source of the necessary input for the series of algorithms that predict impact burial of cylinders in the seafloor.

Interrelations between the variations in pitch and vertical velocity have been alluded to in Sections III-B and III-C. Careful observation of the individual trajectories reveals that a certain periodicity may exist in the patterns of the fall of large heavy cylinders as tested in this paper. It appears that after the initial conditions no longer influence the behavior of the free-falling body, the nose-heavy cylinders undergo repeated cycles of changing pitch angle, which in turn directly influences the fall velocity. Thus, cylinders assume an almost horizontal orientation with immediate and often significant drop in the vertical component of velocity, followed by the sudden increase in the rotational velocity (in the vertical plane of the mine). This rather abrupt downward pitching of the nose results in an acceleration of the cylinder in the downward direction again. It appears that these patterns exist for all nose configurations and for all the CMOs tested. The more nose-heavy the cylinder, the more pronounced is this effect. None of our experiment locations had depth quite sufficient to remove all doubts about the periodic nature of this behavior. At the maximum depth tested (25 m), the cylinders seemed to go through no more than 1.5 of these cycles. Only tests at possibly 100 m or more would prove or disprove the existence and the frequency of these cycles.

B. Significance of the Nose Geometry

The influence of the nose geometry on the behavior of the cylinders in free-fall has been discussed and illustrated in Fig. 3–12 and summarized in Table II. It appears that the blunt configuration is the most stable of the three tested. Most of the time, the chamfered shape proved to be the least stable. This refers to the existence of the quasi-stable conditions of the various dynamic variables, in the mean sense.

Another interesting observation was made when comparing the behavior of the different shapes during air releases. A cylinder released in the air entraps air upon water entry that forms a bubble envelope around the accelerating body. This bubble envelope has a pronounced effect on the time needed to achieve the quasi-stable conditions. It has a reduced friction

TABLE II
MEAN AND STD VALUES FOR ALL VARIABLES MEANS IN QUASI-STABLE MODE, GROUPED ACCORDING TO CMO, NOSE GEOMETRY, AND RELEASE PITCH

Variable	CMO	Nose geometry	Release pitch, °	Mean	STD
mean(Vz), m/s	0.05	all	all	3.87	0.68
	0.02	all	all	3.47	0.34
	0.05	blunt	all	3.72	0.67
	0.02	blunt	all	3.46	0.36
	0.05	hemi	all	3.72	0.54
	0.02	hemi	all	3.47	0.30
	0.05	chamf	all	4.14	0.69
	all	blunt	31	3.55	0.62
	all	blunt	5	3.46	0.36
	all	blunt	0	3.86	0.69
	all	hemi	31	3.60	0.65
	all	hemi	5	3.47	0.30
	all	hemi	0	3.85	0.37
	all	chamf	31	4.19	0.65
	all	chamf	0	3.95	0.60
mean(Vx'), m/s	0.05	all	all	1.52	0.56
	0.02	all	all	0.35	0.62
mean(pitch), °	0.05	all	all	32.8	16.6
	0.02	all	all	0.2	8.4
	all	blunt	31	27.1	17.4
	all	blunt	5	2.3	6.9
	all	blunt	0	38.3	15.1
	all	hemi	31	29.6	21.3
	all	hemi	5	-1.6	8.0
	all	hemi	0	27.6	12.1
	all	chamf	31	35.7	13.5
	all	chamf	0	32.6	14.9
mean(pitch rate), °/s	0.05	all	all	3.6	20.2
	0.02	all	all	-2.2	12.4
	all	blunt	31	1.9	12.7
	all	blunt	5	0.6	10.5
	all	blunt	0	3.9	15.1
	all	hemi	31	10.7	31.7
	all	hemi	5	-4.6	12.1
	all	hemi	0	4.3	13.9
	all	chamf	31	-1.0	18.6
	all	chamf	0	4.3	21.3

Notes: Vz - vertical velocity, positive downward
Vx' - horizontal velocity in the plane of the cylinder, positive forward
Pitch=0° - horizontal
plane of cylinder = plane of {vertical, cylinder's long axis}
CMO=(CM-CV)/L - center of mass offset ratio
averaging time for all mean values: [1.2 - 4.0] s

on the body and therefore reduced drag, allowing the cylinder to achieve higher initial velocities. After some fall distance, this air envelope dissipates, increasing the overall drag on the body and allowing for the full spectrum of the hydrodynamic effects to take over. The time it took for this bubble envelope to dissipate varied, however, dependent on the release angle and the nose geometry. The blunt configuration was able to retain this air-bubble envelope the longest, especially during inclined releases (31° nose down). In all cases, after about 1.2 s into the fall on average, these initial condition-dependent influences ceased, and the cylinder could be considered to have attained a quasi-stable state.

C. Influence of the CMO

The change in the CMO in the cylinder had profound influence on its dynamics. This was observed earlier on very small model cylinders in pool tests [1], [2] and tests of one-third scale models [9]. The results of our experimental study on full size cylinders confirm this dependence. The tests with larger CMO attain higher vertical velocities with higher variance as a result of increased variability in orientation. On the other hand, drops with more centrally weighted cylinders attained the more hydrodynamically stable position of normality to the incident water flow, producing much smaller variability in velocities and orientations. The STDs for most of these dynamic variables for bodies with CMO = 0.02 were about half of those for CMO = 0.05. On the other hand, and as a result of this behavior, the more centrally weighted cylinders were able to traverse larger lateral distances from the point of release because of their increased stability in free-fall than the more nose-heavy ones.

V. Conclusion

This paper presents results on four test series of large free-falling cylinders with variable nose geometry, release conditions, and CMO. It was observed that the CMO plays an important role in determining the dynamics of the body in free-fall. The more centrally weighted cylinders tended to reach more stable orientation and maintain that orientation longer throughout the fall. This resulted in slower downward fall velocities and smaller variance in pitch and pitch rate. The calculated STDs of these variables for cylinders with smaller CMO tended to be half of those of the more nose-heavy cylinders. The more even-weighted cylinders also displayed the capacity for larger lateral travel from the deployment point, as a result of the added hydrodynamic stability throughout the fall.

Influence of nose shape had lesser effect compared to CMO effects. In general, the blunt nose shape displayed the least erratic behavior, and the chamfered nose—the most. It was also observed that the release conditions only influenced the behavior of the cylinders for the initial 1.2–1.5 s. From that point on, the cylinders appeared to reach a quasi-stable state in the mean sense, albeit with strong deviations about the mean, as evidenced by large calculated STD values.

The information collected and analyzed in this paper is most useful in evaluating and validating a variety of complex hydrodynamic models of free-falling cylinders. The statistical results collected can also be used in driving directly the models for predicting the penetration of the sea bottom sediments by these cylinders. This knowledge is of great importance to the U.S. Navy and also has applications in the Homeland Security field.

Acknowledgment

The authors would like to thank C. Kennedy, C. King, C. Vaughn, G. Bower, M. Richardson, K. Briggs, R. Ray, all U.S. Naval Research Laboratory (NRL) staff, and the captains and crews of R/V Pelican (Cocodrie, LA) and R/V Gyre (Corpus Christi, TX), and many others.

References

[1] P. C. Chu, A. F. Gilles, C. W. Fan, J. Lan, and P. Fleischer, "Hydrodynamics of falling cylinder in water column," *Adv. Fluid Mech.*, vol. 4, pp. 163–181, 2002.

[2] A. F. Gilles, "Mine drop experiments (MIDEX)," M.Sc. thesis, Dept. Oceanogr., Naval Postgraduate School, Monterey, CA, 1993.

[3] Y. Kim, Y. Liu, and D. K. P. Yue, "Motion dynamics of three-dimensional bodies falling through water," *J. Fluid Mech.*, to be submitted for publication.

[4] P. C. Chu, A. Evans, A. Gilles, A. Smith, and V. Taber, "Development of the Navy's 3D mine impact burial prediction model (IMPACT35)," in *Proc. 6th Int. Symp. Technol. Mine Problem*, Monterey, CA, May 10–13, 2004, pp. 1–10.

[5] A. V. Abelev, P. J. Valent, N. G. Plant, and K. T. Holland, "Evaluation and quantification of randomness in free-fall trajectories of instrumented cylinders," in *Proc. MTS/IEEE Conf. OCEANS Mar. Technol. Ocean Sci.*, San Diego, CA, Sep. 22–26, 2003, pp. 2355–2365.

[6] A. V. Abelev and P. J. Valent, "Dynamics of bottom mine burial in soft sediments: Experimental evidence and predictions," in *Proc. Mine Countermeasures Demining Conf. Asia-Pacific Issues MCM in Wet Environments*, Canberra, Australia, Feb. 9–11, 2004, Australian Defence Force Academy, CD-ROM.

[7] S. J. Griffin, J. Bradley, M. D. Richardson, K. B. Briggs, and P. J. Valent, "NRL mine burial experiments," *Sea Technol.*, vol. 42, no. 11, p. 21, 2001.

[8] S. Theophanis, "Accelerometer and fiber optic gyro measurements of an instrumented cylinder used to study impact burial," in *Proc. MTS/IEEE Conf. OCEANS*, Biloxi, MS, Oct. 29–31, 2002, pp. 92–97.

[9] K. T. Holland, A. W. Green, A. V. Abelev, and P. J. Valent, "Parameterization of the in-water motions of falling cylinders using high-speed video," *J. Exp. Fluids*, vol. 37, pp. 690–700, 2004.

Andrei V. Abelev received the M.Sc. and Ph.D. degrees in civil engineering with expertise in soil mechanics from The Johns Hopkins University, Baltimore, MD, in 2001.

He has been a Research Scientist at the U.S. Naval Research Laboratory (NRL) since 2005. He conducts experimental, theoretical, and numerical studies of behavior and structure of marine sediments under various loading conditions, including impact loading and long-term deformations. Before joining the NRL, he worked as a Research Scientist at the University of Southern Mississippi, Stennis Space Center.

Philip J. Valent received the Ph.D. degree in civil engineering with minor in soil mechanics from the Purdue University, West Lafayette, IN, in 1979.

He has been a Research Scientist at the U.S. Naval Research Laboratory (NRL) since 1983, combined with the dual hat of Associate Superintendent of the NRL's Marine Geosciences Division since 1989. He has worked on the design and testing of foundation and anchor systems for deep ocean, systems for sequestering of high-level radioactive wastes and contaminated dredged material on the deep seafloor, and prediction of impact burial of objects in seabed sediments.

Dr. Valent is a member of the American Society of Civil Engineers (ASCE).

K. Todd Holland received the M.S. and Ph.D. degrees in marine geology from the Oregon State University, Corvallis, in 1992 and 1995, respectively.

He has been a Project Scientist at the U.S. Naval Research Laboratory (NRL) since 1995 studying near-shore dynamics and littoral applications of video techniques. Before joining the NRL, he worked as an Oceanographer with the U.S. Geological Survey, Reston, VA.

Dr. Holland is a member of the American Geophysical Union (AGU).